Malaysian Journal of Civil Engineering 29(3):250-272 (2017)

SEISMIC SAFETY EVALUATION OF ABDUL MANNAN OVERPASS IN CHITTAGONG, BANGLADESH

M. A. Rahman Bhuiyan[1*] & Hafizul Alim[2]

[1] *Department of Civil Engineering, Chittagong University of Engineering and Technology Chittagong 4349, Bangladesh*
[2]*Department of Civil Engineering, Lamar University, USA*

*Corresponding Author: *arbhuiyance@cuet.ac.bd*

Abstract: A number of multi-span overpasses in major cities of Bangladesh, such as Dhaka (the capital city) and Chittagong (the principal seaport city) have been constructed for the last few years with a view to reducing the traffic congestion at critical junctions. Abdul Mannan overpass is one of these, which is located in Chittagong city. It has been launched in the year of 2012 with a prime objective of reducing the traffic congestion within Chittagong city. This study is devoted towards assessing seismic safety of this overpass, which comprises in two phases: the first phase is dedicated towards the evaluation of seismic lateral strength and ductility whereas the second phase is aimed at assessing seismic fragility and retrofit of the overpass. In this regard, the first phase utilizes the ductility method as suggested by Japan Road Association (JRA) to evaluate lateral strength and ductility of piers of the overpass considering their different modes of failure. The lateral strengths of pier sections in bending are obtained based on their nonlinear sectional analyses results, while the shear strengths are estimated using JRA suggested method. The fiber models with conventional constitutive models for concrete and steel are used to obtain the moment-curvature relationships at critical sections of the overpass pier. The pushover analysis method is employed to derive the force-displacement relationships of piers using the results of the moment-curvature relationships. Subsequently, the lateral seismic demand, allowable lateral force, yield displacement, ultimate displacement and displacement ductility are obtained using the standard methods. In the second phase, the nonlinear dynamic analysis of a typical pier of the overpass is carried out for seismic fragility assessment followed by an assessment of seismic retrofit strategy suitable for the overpass. The numerical results of the study indicate that most of the piers of the overpass do not comply seismic safety requirements for design earthquake ground motion rerecords, which warrants the retrofit of piers of the overpass.

Keywords *Lateral strength, ductility, pushover analysis, moment-curvature relationship, force-displacement relationship, retrofit, fragility.*

1.0 Introduction

Bridge, in general, is a structure that crosses over a body of water, traffic or other obstructions permitting smooth and safe passage of vehicles. There are several forms of bridges which are widely used in transportation systems. Overpass, one of different bridge forms, is an elevated structure carrying highway over roads, railways and other features. So, in the subsequent discussion of this paper, the terms '*bridge*' and '*overpass*' are synonymously used. A number of overpasses are being constructed in Dhaka and Chittagong metropolitan cities of Bangladesh with a view to reducing the traffic congestions. One of these is the Abdul Mannan overpass located in Chittagong, which has been open for traffic in 2012. This kind of structure plays very important role for evacuation and emergency routes for rescues, first aid, medical services, fire-fighting and transporting urgent disaster commodities. In view of importance of life line structures in transportation network, it is the key issue to minimize as much as possible loss of the bridge functions during earthquakes.

Bangladesh lies within a seismically active zone. Due to the country's position adjacent to the very active Himalayan front in the north and Burma deformation front in the east expose it to strong shaking from a variety of earthquake sources that can produce large magnitude of earthquakes (Ali and Chowdhury, 1992). It is reported that the potential for magnitude 8 or greater earthquakes on the nearby Himalayan and Burmese fronts is very high (Akhter, 2010). It is worthwhile to mention that this kind of overpasses is one of the most critical components of transportation network systems. So, it is indispensable to evaluate the seismic vulnerability of the overpass. The vulnerability assessment of this kind of structure is widely recognized to be useful for prioritization of seismic retrofitting decisions, disaster response planning, estimation of direct monetary loss, and evaluation of loss of functionality in the event of an earthquake.

Several seismic codes and standards, such as JRA (2002), CalTrans (1999), Eurocode (1998), AASHTO (2002), have been developed to evaluate seismic safety of bridge structures. The main philosophy lies in seismic safety evaluation that the structures shall resist earthquakes of small to moderate magnitudes without damage while for the large magnitude earthquake excitations the reparability and no collapse condition of the structures shall be ensured. In this case, the structures are allowed to undergo large deformations showing nonlinear behavior and energy dissipation for minimizing the losses.

The seismic vulnerability of bridge structure is usually expressed in the form of fragility curves, which display the conditional probability that the structural demand (structural response) caused by various levels of ground motion intensity exceeds the structural capacity defined by a damage state. Recognition of the usefulness of the vulnerability information in assessing, managing, and reducing seismic risk has resulted in

development of different fragility-curve generation methodologies involving probabilistic seismic performance evaluation of bridges like structures, such as overpass. Some of these methodologies are expert opinion-based (ATC, 1985), some are empirically formulated based on observed damage from past earthquakes (Basoz and Kiremidjian, 1998; Yamazaki *et al.*, 2000), while others are derived from analytical simulation methods (Alam *et al.*, 2012; Bhuiyan and Alam, 2012; Billah *et al*., 2013; Choi *et al.*, 2004; Hwang *et al.*, 2000, 2001; Karim and Yamazaki, 2001; Nielson and DesRoches, 2007a, b; Padgett and DesRoches, 2008). Though all of the methodologies have their own limitations in evaluating the probabilistic seismic performance of bridge like structure, fragility assessment methodologies using analytical approaches have become widely adopted since they are more readily applicable to bridge types and geographical regions where seismic bridge damage records are insufficient. Moreover, empirical vulnerability analyses are virtually impossible for Bangladesh, since structural damage data due to earthquakes are not available.

On the basis of the background, the study aims at assessing seismic safety of an overpass. In this regard, the seismic lateral strength and ductility of piers are evaluated using JRA suggested method followed by assessing the seismic fragility and retrofit strategy of the overpass. The lateral strengths in bending are obtained using the results of nonlinear sectional analyses of the pier sections, while the shear strength of the piers are estimated using JRA (2002) defined equations taking into account the effect of depth, volumetric ratio of lateral steel, crushing strength of concrete and yield strength of steel. The fibre models with conventional constitutive models for concrete and steel of the pier sections at critical locations are developed to obtain the moment-curvature relationships. The nonlinear pushover analyses of the piers are carried out to obtain force-displacement relationships. The material nonlinearity is considered in the sectional analysis whereas both material and geometric nonlinearity are considered in the pushover analysis. The lateral seismic force, allowable lateral force, yield displacement, ultimate displacement and displacement ductility are obtained from force-displacement relationships of the piers. Moreover, the nonlinear dynamic analysis of a typical pier of the overpass is carried for seismic fragility assessment of the overpass. Finally, an assessment of seismic retrofit strategy suitable for the overpass has been carried out. The numerical results of the study indicate that most of the piers of the overpass do not remain in compliance with the seismic safety requirements for design earthquake ground motion rerecords, which warrants the retrofit of piers of the overpass.

2.0 Description of the Overpass

Chittagong is the second largest and the principal seaport city in Bangladesh. Chittagong city is surrounded by many primary and secondary road networks. For improvement of

traffic network, the city development authority is taking many initiatives in order to reduce the traffic congestion within the city. However, there is a debate among the town planners, city dwellers and the professionals who are working in the area of transportation planning, regarding the effectiveness of the overpass in reducing the traffic congestion in the city area. As a part of the initiatives, a 1331.60 m long overpass over the national highway (N1) connecting CDA (Chittagong Development Authority) Avenue road and Shah Amanat Bridge (i.e., it is one of the most important connecting passageways between Cox's Bazar sea beach and the rest of Bangladesh) approach road has been launched in the year of 2012 over the Bahaddarhat Intersection. The Bahaddarhat Intersection is a place in Chittagong city where N1 national highway meets with Chittagong-Cox's Bazar Highway (Figure 1 (a)). There are 25 spans of variable lengths excluding the two approach roads at both ends of the overpass. The span length of the overpass varies from 35 m to 42 m. The length of each approach road located at the ends of the overpass is 165.3 m. The deck of the overpass comprises six to seven pre-stressed concrete girders with 200 mm reinforced concrete slab including asphalt wearing course. The girders rest on elastomeric rubber pad installed at top of each pier and abutment, which form a multi-span simply supported bridge structure. There are 24 piers having variable heights ranging from 3.65 m to 7.29 m with two abutments at its ends. The longitudinal layout and transverse section of the overpass are given in Figure 1 (b). The geometric dimensions of deck, piers and re-bar details of a typical pier are presented in Figure 2 and Table 1. Relevant material properties of the overpass are presented in Table 2. The general elevation and sectional details of the overpass are presented in Figure 2.

Table 1: Height, cross-section and re-bar details of piers of the overpass

Pier No.	*Pier height(m)*	*Cross-sectional diameter (m)*	*Longitudinal reinforcement*
1	3.65	2.5	72-φ32 mm
2	4.92	2.5	72-φ32 mm
3	5.86	2.5	72-φ32 mm
4	6.56	2.5	72-φ32 mm
5-21	7.29	2.5	72-φ32 mm
22	7.06	2.5	72-φ32 mm
23	5.42	2.5	72-φ32 mm
24	4.15	2.5	72-φ32 mm

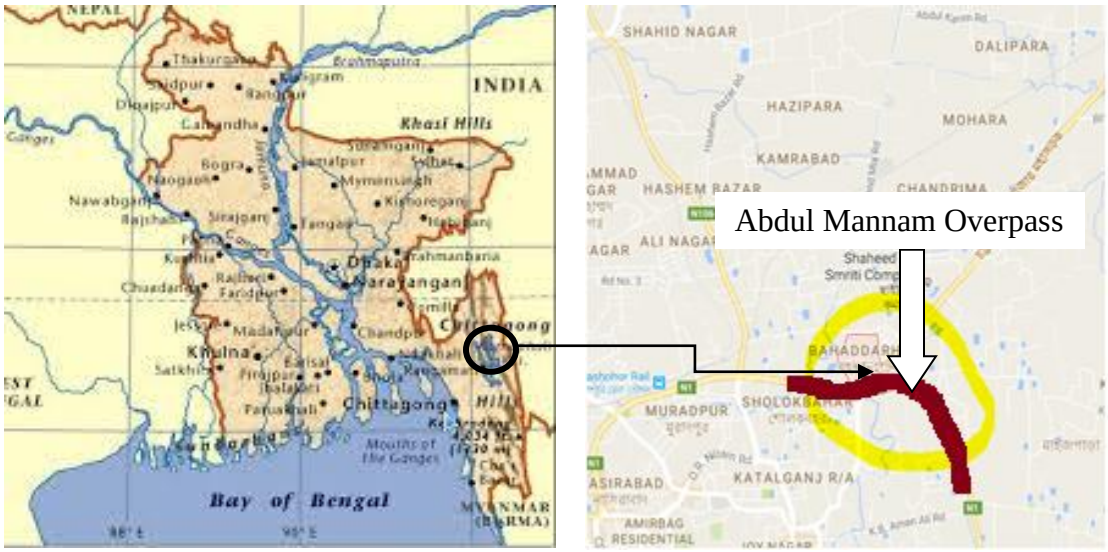

(a) Location of the overpass

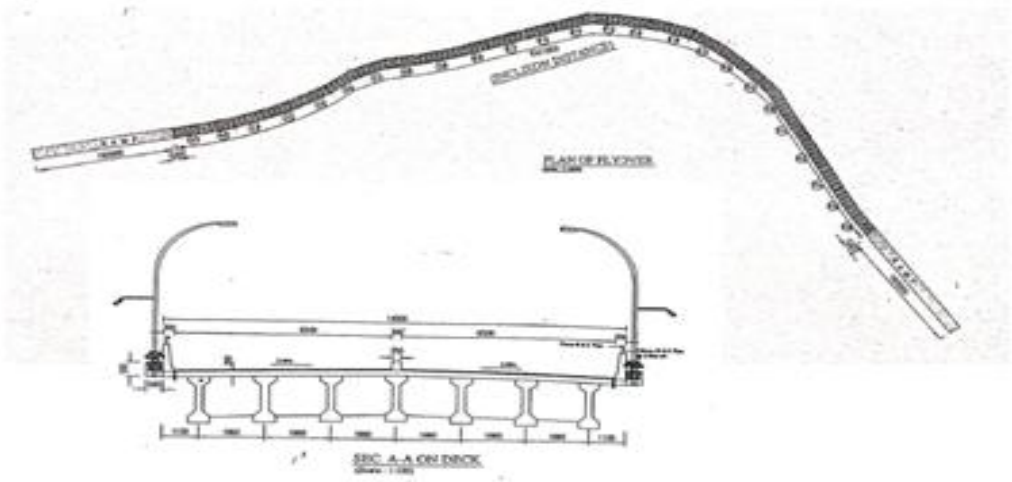

(b) Longitudinal layout and transverse section of the overpass

Figure 1:Location and geometric details of the overpass
(*Photo Courtesy: Chittagong Development Authority*)

Table 2: Material properties of the overpass

Material Name	*Description of material properties*	
Unconfined concrete	Compressive strength (MPa)	35.0
	Tensile strength (MPa)	3.0
	Ultimate strain	0.003
	Confinement factor	1.0
	Specific gravity	24
Confined concrete	Compressive strength (MPa)	35.0
	Tensile strength (MPa)	3.0
	Ultimate strain	0.0035
	Confinement factor	1.2
	Unit weight (kg/m^3)	2400
Steel	Yield strength (MPa)	414
	Modulus of elasticity (MPa)	200000
	Strain hardening parameter	0.0075
	Fracture strain	0.06
	Unit weight (kg/m^3)	7800

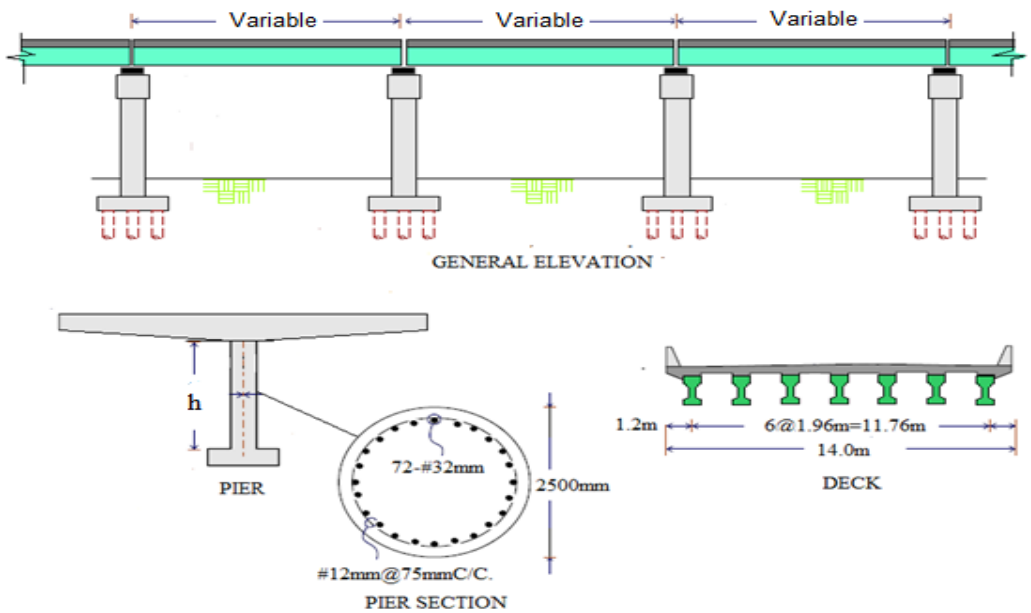

Figure 2: General elevation and sectional details of the overpass

3.0 Lateral Strength and Ductility of the Overpass

Evaluation of adequacy of a pier of bridge structure to withstand imposed seismic loads requires assessment and comparison of anticipated demand and available capacities. In this regard, the lateral strength, ductility and mode of failure of piers are computed using the method of nonlinear static analysis (i.e., pushover method) and the analytical method suggested by Japan Road Association (JRA, 2002). In addition, a numerically solved nonlinear analysis program is used to conduct the pushover analysis in order to derive the force-displacement relationship of a pier. In this connection, a sectional analysis (Response, 2000) has been carried out to derive moment-curvature relation at each section of a pier of the overpass.

3.1 Development of Force-Displacement Relationship

The force-displacement relationship of piers is derived from the results of moment-curvature relation at each section as obtained from sectional analysis (Alim, 2014). Sectional properties of the piers are related to the characteristics of the materials i.e., stress-strain relationship and strength of materials. Different models of concrete are developed for seismic analysis (Park *et al.*, 1985; Madas and Elnashai, 1992; Spoelstra *et al.*, 1999). A concrete model developed by Hoshikuma *et al.* (1997) is used in this work. The descending branch of the concrete constitutive relationship as well as the increase of strength and corresponding strain because of confinement effect is taken into account as shown in Figure 3 (a). The nonlinear model for reinforcing steel is used in the study and the constitutive model is shown in Figure 3 (b).

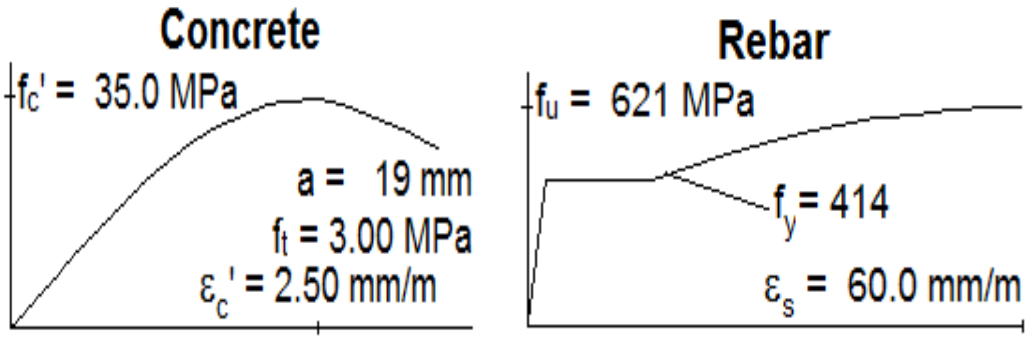

(a) (b)

Figure 3: Constitutive model of materials (a) Concrete and (b) Steel

The stress-strain curve of concrete consists of three parts i.e., an ascending branch, falling branch, and sustaining branch as shown in Figure 3(a). The stress-strain curve can be expressed as:

$$f_c = \begin{cases} E_c\varepsilon_c\left\{1-\frac{1}{n\left(\frac{\varepsilon_c}{\varepsilon_{cc}}\right)}\right\} \ (0 \le \varepsilon_c \le \varepsilon_{cc}) \\ fcc\left\{1-E_{des}\left(\frac{\varepsilon_c}{\varepsilon_{cc}}\right)\right\} \ (\varepsilon_{cc} \le \varepsilon_c \le \varepsilon_{cu}) \end{cases}, \quad (1)$$

where, n is coefficient and E_{des} is the deterioration rate, are given as,

$$n = E_c\varepsilon_{cc} \Big/ \left(E_c\varepsilon_{cc} - \sigma_{cc}\right) \quad (2)$$

$$\sigma_{cc} = \sigma_{c0} + 3.8\alpha\rho_s\sigma_{sy}; \varepsilon_{cc} = 0.002 + 0.033\beta\frac{\rho_s\sigma_{sy}}{\sigma_{c0}} \quad (3)$$

$$E_{des} = 11.2\frac{\sigma_{c0}^2}{\rho_s.\sigma_{sy}} \quad (4)$$

where, σ_{c0} is design strength of concrete, $\sigma_{sy}$is the yield strength of reinforcement, α and β are shape factors and ρ_s is the volumetric ratio of tie reinforcements. The ultimate displacement d_u is defined as displacement at the gravity centre of superstructure when the concrete compression strain at out-most reinforcements reaches the following ultimate strain, ε_{cu}

$$\varepsilon_{cu} = \begin{cases} \varepsilon_{cc} & type-I \quad earthquake \\ \varepsilon_{cc} + 0.2\sigma_{cc} \Big/ E_{des} & type-II \quad earthquake \end{cases} \quad (5)$$

where, α and β are modification factors depending on confined sectional shape: for circular section β = 1.0 and α = 1.0; for square section β = 0.2 and α = 0.4. To obtain the force-displacement relationship at top of pier, the pier is divided into 50 slices (as recommended in JRA (2002)) along its height. A sectional analysis of a pier section of the overpass is conducted to derive moment-curvature relation (Figure 4).

Finally, the force displacement relationship at the top of the bridge pier is obtained using the moment-curvature relation (Figure 4) and shear stress-strain diagram (Figure 3). The lateral load–displacement characteristics of piers of the overpass as obtained from the pushover analysis are presented in Figure 5. The force-displacement relationship of each pier shows a similar fashion with different yield, ultimate lateral loads and deformations. The yield, ultimate deformations of the piers along with their failure modes have been used to compute the allowable ductility of the piers. The failure modes of the piers are evaluated based on their bending and shear capacities, which subsequently helps compute the allowable ductility of the piers

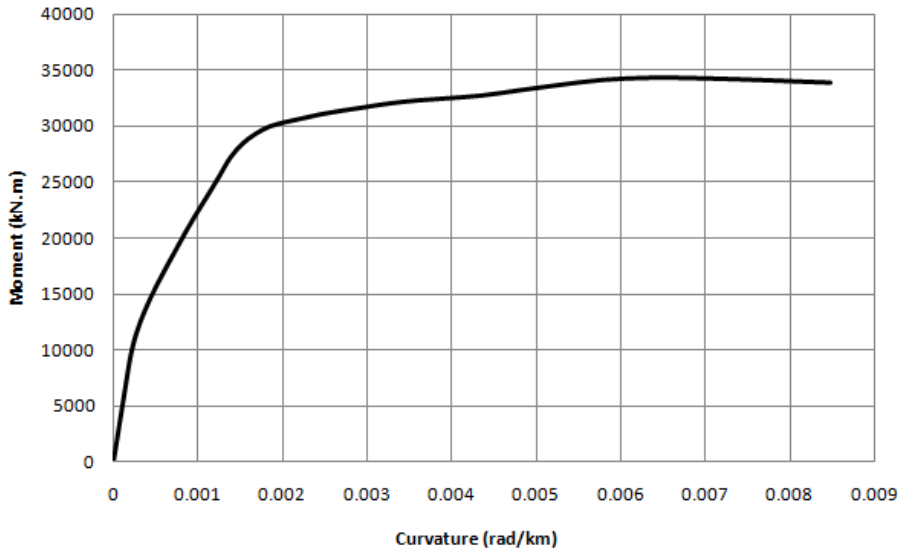

Figure 4 Moment-curvature relation of a typical pier section of the overpass

3.2 *Evaluation of Seismic Load, Lateral Strength, Ductility and Failure Mode of Piers*

Ductility and lateral strength of each pier are evaluated considering its shear and flexural capacities and failure mode. Eqs. (6) to (8) illustrate the ways of evaluating the failure mode, lateral strength and allowable ductility of each pier.

$$\text{Failure Mode} = \begin{cases} \text{flexural failure} \ldots\ldots\ldots\ldots\ldots\ldots\ldots\ldots\ldots\ldots\ldots\ldots\ldots\ldots p_u \le p_s \\ \text{shear failure after flexural damage} \ldots\ldots\ldots\ldots p_u \le p_{so} \\ \text{shear failure} \ldots\ldots\ldots\ldots\ldots\ldots\ldots\ldots\ldots\ldots\ldots\ldots\ldots\ldots\ldots p_u \ge p_{so} \end{cases} \quad (6)$$

The lateral capacity $P_a$and the allowable displacement ductility factor $\mu_a$are given as,

$$p_a = \begin{cases} p_u \ldots \text{flexural failure} + \text{shear failure after flexural damage} \\ p_{so} \ldots\ldots\ldots\ldots\ldots\ldots\ldots\ldots\ldots\ldots\ldots\ldots\ldots\ldots\ldots\ldots\ldots\ldots\ldots\ldots\ldots \text{shear failure} \end{cases} \quad (7)$$

$$\mu_a = \begin{cases} 1 + \dfrac{\delta u - \delta y}{\alpha \delta y} \ldots\ldots\ldots\ldots\ldots\ldots\ldots\ldots\ldots\ldots\ldots\ldots \text{Flexural failure} \\ 1 \ldots\ldots\ldots\ldots\ldots\ldots\ldots\ldots\ldots\ldots\ldots\ldots\ldots\ldots\ldots\ldots\ldots\ldots\ldots\ldots \text{Shear failure} \end{cases} \quad (8)$$

where which α = safety factor depending on importance of bridges and the type of ground motion (α = 3.0 and 2.4 for important and ordinary bridges, respectively, under the far field ground motions, and α = 1.5 and 1.2 for important and ordinary bridges,

respectively, under the near fault ground motions), δ_y and δ_u= yielding and ultimate displacements of the pier, which are defined in (Figure 6). The yield and ultimate displacements, mode of failure and allowable displacement ductility of piers of the overpass have been obtained using their lateral force-displacement relationships shown in Figure 5 and Eqs. (7) and (8) as presented in Table 3.

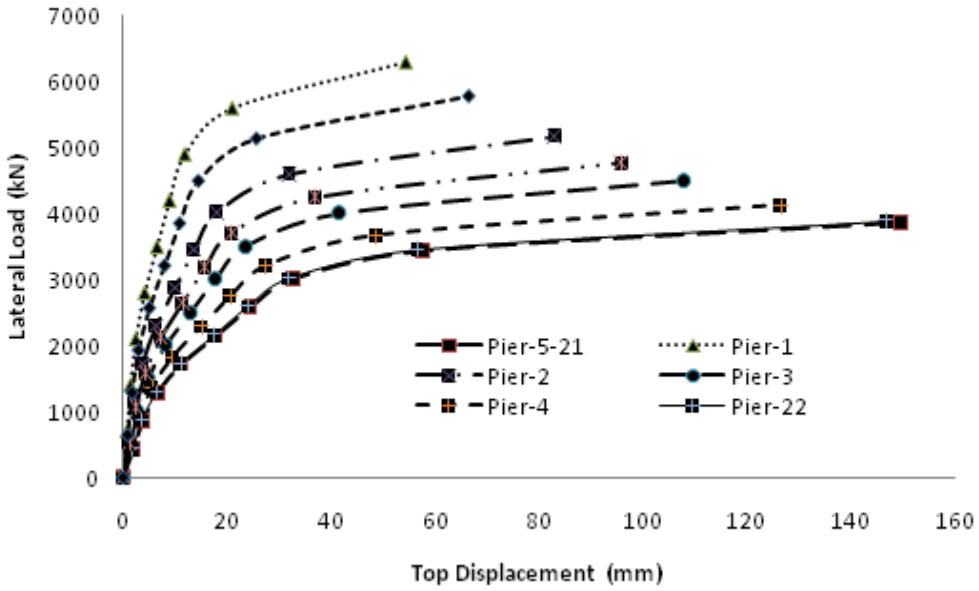

Figure 5: Force-displacement relationships for piers of the overpass as obtained from pushover analysis

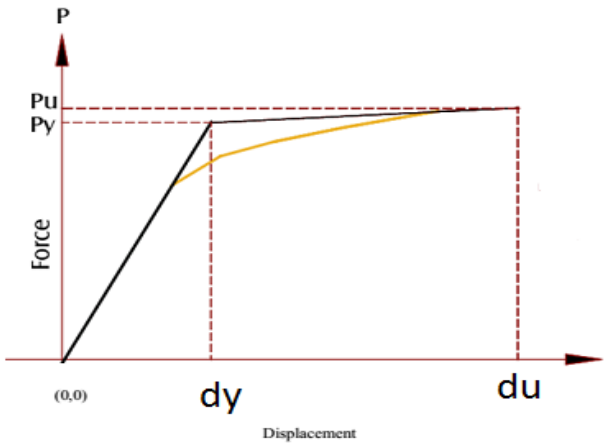

Figure 6: Definition of yield and ultimate displacements from the push-over analysis result of a pier

Table 3: Mode of failure and ductility of the overpass piers

Pier No	*Pier height (m)*	*Yield displacement, δ_y (mm)*	*Ultimate displacement, δ_u (mm)*	*Safety factor, α*	*Mode of failure*	*Allowable displacement ductility, μ_a*
1	3.653	12.00	54.26	3.0	Shear	1.00
2	4.917	15.00	83.10	3.0	Bending	2.51
3	5.857	25.00	107.98	3.0	Bending	2.11
4	6.557	28.00	126.41	3.0	Bending	2.17
5 to 21	7.290	25.00	149.55	3.0	Bending	2.66
22	7.057	28.00	146.82	3.0	Bending	2.41
23	5.417	20.00	95.93	3.0	Bending	2.27
24	4.153	12.00	66.43	3.0	Shear	1.00

3.3 Seismic Safety Assessment of the Overpass

The seismic safety of the pier can be estimated such that the lateral load capacity P_a of the pier must be greater than or equal to the lateral load demand during seismic excitations,

$$P_a \geq \frac{S_s \cdot W}{g \cdot R} \tag{9}$$

where S_s is the elastic response acceleration, W is the tributary weight and R is the response modification factor which can be assumed as,

$$R = \sqrt{2\mu_a - 1} \tag{10}$$

Shear strength of concrete can be calculated by following equations (JRA, 2002),

$$P_s = S_c + S_s \tag{11}$$

$$S_c = C_c C_e C_{pt} f'_c bd \tag{12}$$

$$S_s = \frac{A_w f_{sy}(sin\theta + Cos\theta)}{1.15a} d \tag{13}$$

where,
P_s = Shear Strength (N)
S_c = Shear Strength resisted by concrete (N)
S_s =Shear Strength borne by hoop tie (N)
a = Spacing of the stirrup (mm)
d = the effective depth of the pier section (mm)

The value of C_e and C_{pt} are given in Table 4 and Table 5.

Table 4: Value of C_e in relation to effective depth d of a pier section (JRA, 2002)

Effective Depth (mm)	*Below 1000*	*3000*	*5000*	*Above 10000*
C_e	1.0	0.7	0.6	0.5

Table 5: Value of C_{pt} in relation to effective depth d of a pier section (JRA, 2002)

Tensile Reinforcement (%)	*0.2*	*0.3*	*0.5*	*Above 1%*
C_{pt}	0.9	1.0	1.2	1.5

Equations (9) to (14) are used to evaluate the seismic safety of the overpass piers. In this case, two peak ground accelerations (i.e., PGA of 0.15g and 0.25g) complying seismic performance requirements of bridge structures in the region of the overpass location. Bangladesh National Building Code (BNBC, 2006) is the only official document, which has been used since 1993 (officially it has been used since 2006) as guidelines for seismic design of building structures. A seismic zoning map has been suggested in BNBC with a design earthquake ground motion having the return period of 200 years. As per the guidelines of BNBC, the total territorial area of Bangladesh has been divided into three seismic zones, namely, very active zone (Zone 3: PGA of 0.25g), moderate active zone (Zone 2: PGA of 0.15g) and low active zone (Zone 1: PGA of 0.075g). Chittagong city is located in moderate active zone (Zone 2: PGA of 0.15g). It is noted that a bridge structure (i.e. overpass) structure shall be designed for higher seismic performance in compared to building (Bhuiyan, 2009). Moreover, the revised version of BNBC (the official version will be published very soon) has suggested that the building structures shall be designed for an earthquake ground motion having a return period of 2475 years and the corresponding PGA values for seismic zones are, 0.36g, 0.28g and 0.12g, respectively. Considering all these aspects two PGA values of 0.15g and 0.25g have been utilized in seismic safety evaluation of the said overpass.

Table 6 shows the lateral strength, failure mode and seismic safety of the overpass for a ground motion records having PGA of 0.15g whereas Table 7 presents those for the overpass subjected to a ground motion records having PGA of 0.25g. Generally, tall piers seem to be vulnerable to flexural failure whereas the relatively short piers are susceptible to shear failure rather than flexural failure. Moreover, the piers of the overpass do not comply the seismic safety requirements for a PGA of 0.25g whereas for a PGA of 0.15g, most of the piers can be considered to be safe except piers 1 and 24.

Table 6: Lateral seismic load, allowable lateral load and seismic safety of the overpass pier for a PGA of 0.15g

Pier No.	*Pier height (m)*	*Lateral seismic load, P_{us} (kN)*	*Allowable lateral load, P_a (kN)*	*Safety status*
1	3.653	6469	5421	Not Safe
2	4.917	3224	4574	Safe
3	5.857	3609	4164	Safe
4	6.557	3538	3839	Safe
5 to 21	7.290	3112	3424	Safe
22	7.057	3306	3475	Safe
23	5.417	3443	4389	Safe
24	4.153	6469	5421	Not Safe

Table 7: Lateral seismic load, allowable lateral load and seismic safety of the overpass pier for a PGA of 0.25g

Pier No.	*Pier height (m)*	*Lateral seismic load, P_{us} (kN)*	*Allowable lateral load, P_a (kN)*	*Safety status*
1	3.653	10781	5421	Not Safe
2	4.917	5373	4574	Not Safe
3	5.857	6015	4164	Not Safe
4	6.557	5897	3839	Not Safe
5 to 21	7.290	5186	3423	Not Safe
22	7.057	5510	3479	Not Safe
23	5.417	5738	4388	Not Safe
24	4.153	10781	5421	Not Safe

4.0 Seismic Fragility Assessment for a Pier of the Overpass

In the preceding sections, it has been observed from the numerical results that all the piers do not comply the seismic load requirements for a PGA of 0.25g whereas for a PGA of 0.15g, most of the piers can be considered to be safe except pier-1 and pier-24. The numerical results as discussed in the preceding sections indicate that all piers of the overpass are required to be retrofitted to carry out the design seismic loads, an earthquake ground motion having a return period of 2475 years. In the subsequent sections, the numerical results of seismic fragility assessment for a typical pier of the pass have been presented and discussed in their as-built and retrofitted conditions. To the end, a pier of 7.290 m height (Table 7) having the cross-sectional details shown in Figure 2 is considered in the analysis. For the retrofit purpose of the piers of the overpass, two retrofit techniques are used: CFRP and concrete jacketing. The CFRP jacketing has the tensile strength of 628 MPa, ultimate axial strain of 10 mm/mm and thickness of 3.42 mm and the concrete jacketing has the compressive strength of 34 MPa, and the ultimate strain of 0.002 and thickness of 150 mm. The concrete jacket is reinforced with 20–25 mm vertical deformed bars with the same properties as those in

the original piers (Table 2). The seismic fragility of the as-built and the retrofitted pier have been evaluated using analytical fragility curves. Many analytical methods are available to derive analytical fragility functions for expressing seismic vulnerability of the bridge structure, which include elastic spectral analyses (Hwang *et al.*, 2000), nonlinear static analyses (Shinozuka *et al.*, 2000), and linear/nonlinear time-history analyses (Hwang *et al.*,2001; Choi *et al.*, 2004; Mackie and Stojadinovic, 2004). In the current work, the nonlinear time-history analysis method has been utlized for generating the fragility curves.

4.1 Analytical Model of An Overpass Pier

The superstructure consisting of RC decks and post-tensioned pre-stressed concrete girders is modeled using linear beam-column elements so that the superstructure remains elastic under the seismic loads applied in the longitudinal direction (Ghobarah *et at.*, 1988). The analytical model of a tributary deck along with a pier (pier-girder system) is shown in Figure 7. The pier-girder system is approximated as a continuous 2-D finite element frame using the SeismoStruct nonlinear analysis program (SeismoStruct, 2011). A finite element model with frame elements is used to approximate the pier-girder system with a finite number of degrees of freedom. The superstructure and substructure of the system are modeled as a lumped mass system divided into a number of small discrete segments. The mass of each segment is assumed to be distributed between two adjacent nodes. The body of the overpass pier is modeled using fiber elements. Each fiber has a stress–strain relationship, which can be specified to represent unconfined concrete, confined concrete, and longitudinal steel reinforcement. The confinement effect of the concrete section is considered on the basis of reinforcement detailing. The bottom end of the overpass pier is considered fully restrained in all directions.

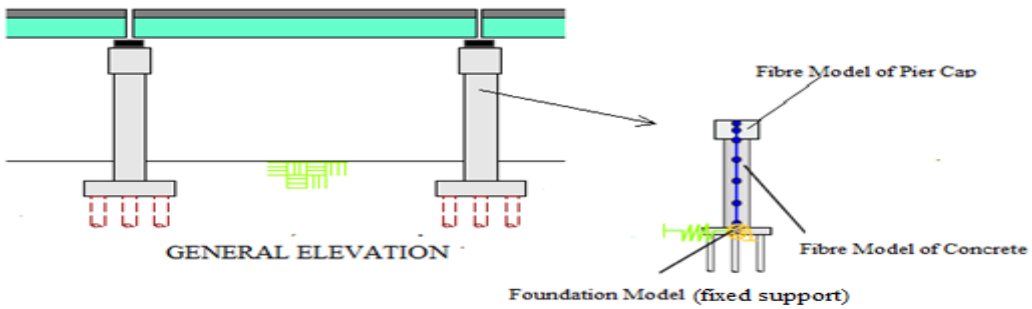

Figure 7: Analytical model of an overpass pier

4.2 Characteristics of Damage States

Damage states for bridge structures should be defined in such a way that each damage state indicates a particular level of structural functionality. A capacity model is needed to measure the damage of bridge structure component based on prescriptive and descriptive damage states in terms of EDPs (Choi *et al.*, 2004). Four damage states as defined by FEMA (2003) are commonly adopted in the seismic vulnerability assessment of engineering structures, namely slight, moderate, and extensive and collapse damages. Bridge piers are one of the most critical components, which are often forced to enter into nonlinear range of deformations under strong earthquakes. In this study, the displacement ductility of the bridge pier is adopted as EDP. Hwang *et al.* (2001) recommended four different damage states for bridge pier (Table 8) based on ductility limit.Moreover, retrofitting of piers affects their seismic demand and capacity. For a retrofitted bridge pier, limit states are obtained by transforming the ductility limit states proposed by Hwang *et al.*(2001) and Billah *et al.* (2013) as given in Table 8.

Table 8: Damage/limit state of bridge component

Damage State ⟶		*Slight (DS=1)*	*Moderate (DS=2)*	*Extensive (DS=3)*	*Damage ((DS=3)*
Bridge Component	Physical Phenomenon	Cracking and Spalling	Moderate cracking and spalling	Degradation without collapse	Failure leading to collapse
As Built Bridge Pier	Displacement Ductility, μ_d	$\mu_d > 1$	$\mu_d > 1.2$	$\mu_d > 1.76$	$\mu_d > 4.76$
CFRP Retrofitted Pier	Displacement Ductility, μ_d	$\mu_d > 1.81$	$\mu_d > 3.89$	$\mu_d > 6.48$	$\mu_d > 12.96$
RCC Jacketing Retrofitted Pier	Displacement Ductility, μ_d	$\mu_d > 1.72$	$\mu_d > 3.7$	$\mu_d > 6.19$	$\mu_d > 12.32$

4.3 Ground Motion Records

A suite of 20 ground motions are used in this study to develop fragility curves for the as-built and retrofitted overpass piers. The characteristics of the earthquake ground motion records are presented in Table 9. All these ground motions have PGA values ranging from 0.24g to 0.728g. Figure 8 shows spectral accelerations and their different percentiles with 5% damping ratio illustrating that the selected earthquake ground motion records are well describing the medium to strong intensity earthquake motion histories.

Table 9: Characteristics of the earthquake ground motion histories

Earthquake No	*Name*	*Recording Station*	PGA_{max} *(g)*	PGV_{max} *(cm/s)*
EQ-1	Northridge	Beverly Hills - Mulhol	0.42	58.9
EQ-2	Landers	Yermo Fire Station	0.24	51.5
EQ-3	Northridge	Canyon Country-WLC	0.40	43.0
EQ-4	Landers	Coolwater	0.28	26
EQ-5	Duzce, Turkey	Bolu	0.70	56.4
EQ-6	Loma Prieta	Capitola	0.53	35
EQ-7	Hector Mine	Hector	0.30	28.6
EQ-8	Loma Prieta	Gilroy Array #3	0.56	36
EQ-9	Imperial Valley	Delta	0.20	26.0
EQ-10	Manjil, Iran	Abbar	0.51	43
EQ-11	Imperial Valley	El Centro Array #11	0.40	34.4
EQ-12	Superstition Hills	El Centro Imp. Co.	0.36	46.4
EQ-13	Kobe, Japan	Nishi-Akashi	0.50	37.3
EQ-14	Superstition Hills	Poe Road (temp)	0.45	35.8
EQ-15	Kobe, Japan	Shin-Osaka	0.20	38.0
EQ-16	Cape Mendocino	Rio Dell Overpass	0.38	43.8
EQ-17	Kocaeli, Turkey	Duzce	0.30	59.0
EQ-18	Chi-Chi, Taiwan	CHY101	0.35	70.6
EQ-19	Kocaeli, Turkey	Arcelik	0.20	17.7
EQ-20	Chi-Chi, Taiwan	TCU045	0.47	36.7

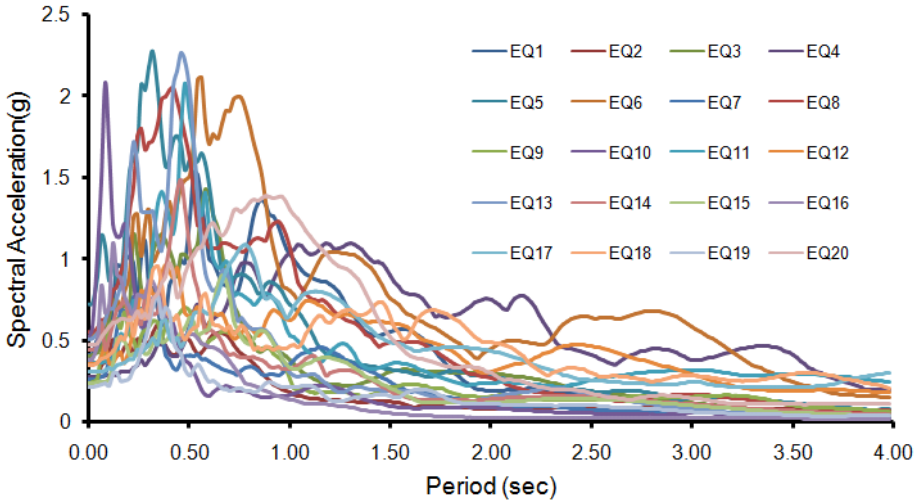

(a) Spectral acceleration

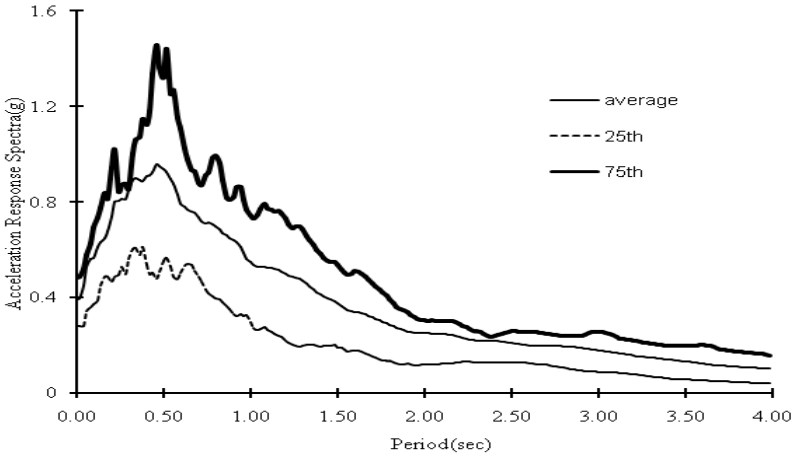

(b) Percentiles of spectral acceleration

Figure 8: Ground motion characteristics

4.4 Generation of Fragility Curves

Fragility function describes the conditional probability, i.e., the likelihood of a structure being damaged beyond a specific damage level for a given ground motion intensity measure. The fragility or conditional probability can be expressed as,

$$\text{Fragility} = P[LS|IM=y] \quad (14)$$

where, LS is the limit state or damage state of the structure or structural component, IM is the ground motion intensity measure and y is the realized condition of the ground motion intensity measure. This study employs Probabilistic Seismic Demand Model (PSDM) to derive the analytical fragility curves using nonlinear time-history analyses of a typical pier. The PSDM establishes a correlation between the engineering demand parameters (EDP) and the ground intensity measures (IM). In this study, the ductility of overpass pier is considered as EDP, and the peak ground acceleration (PGA) is utilized as intensity measure (IM) of each ground motion record. The ground motions are scaled to selective intensity levels and an incremental dynamic analysis (IDA) is conducted at each level of the intensity. The power law function (Cornell *et al.*, 2002), which gives a logarithmic correlation between median EDP and selected IM is given as,

$$EDP = a\,(IM)^b \text{ or, } ln\,(EDP) = ln\,(a) + b\,Ln\,(IM) \tag{15}$$

where, *a* and *b* are unknown coefficients which can be estimated from a regression analysis of the response data collected from the nonlinear time history analysis. The dispersion of the demand, $\beta_{EDP|\,IM}$, conditioned upon the IM can be estimated from Eq. (16).

$$\beta_{EDP|IM} = \sqrt{\frac{\sum_{i=1}^{N}(\ln(EDP) - \ln(aIM^b))^2}{N-2}} \tag{16}$$

With the probability seismic demand models and limit states corresponding to various damage states, it is now possible to generate the fragility function using Eq. (17),

$$P[LS|IM] = \varphi\left[\frac{\ln(IM) - \ln(IM_n)}{\beta_{comp}}\right] \tag{17a}$$

$$\text{and } \ln(IM_n) = \frac{\ln(S_c) - \ln(a)}{b} \tag{17b}$$

$\ln(IM_n)$ is defined as the median value of the intensity measure for the chosen damage state, *a* and *b* are the regression coefficients of the PSDMs and the dispersion component is presented using Eq. (18).

$$\beta_{comp} = \frac{\sqrt{\beta_{EDP|IM} + \beta_c^2}}{b} \tag{18}$$

where β_c is the dispersion value for the damage states of the bridge pier. The parameters of the PSDM are given in Table 10.

Table 10: PSDM parameters

Pier Condition	*ln a*	*b*	$\beta_{EDP\mid IM}$
As-built	1.50	1.19	0.47
FRP Retrofitted	0.98	0.954	0.43
Concrete Jacketed Retrofitted	1.36	1.19	0.45

4.5 Results and Discussion

The fragility curves of a typical overpass pier are derived using Eqs. (14)-(18). Two techniques of retrofit, such as FRP and concrete jacketing, are considered in deriving the fragility curves of the overpass pier in addition to its *as-built* condition. The fragility curves thus derived are presented in Figs.9 (a) to (d), illustrating the relative vulnerability of the overpass pier in '*as built*' and '*retrofitted*' conditions for different damage states. In general, the '*retrofitted*' overpass pier has shown less susceptibility for each damage state in compared to that in '*as built*' condition, as shown in Figs. 9 (a) to (d). For each damage state of the overpass pier, the concrete jacketed pier has shown the higher damage susceptibility in compared to the FRP jacketed pier, at each level of ground motion intensity. In particular, the FRP and concrete jacketed overpass piers do not experience extensive and collapse states of damage, for the two ground motion intensities (PGAs of 0.15g and 0.25g, as considered in the safety assessment of the overpass); however, a considerable damage is seen to have incurred in the '*as built*' overpass.

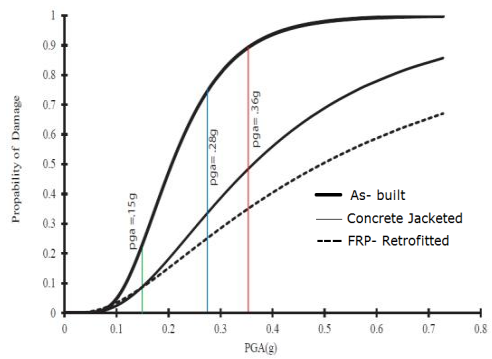

(a) slight

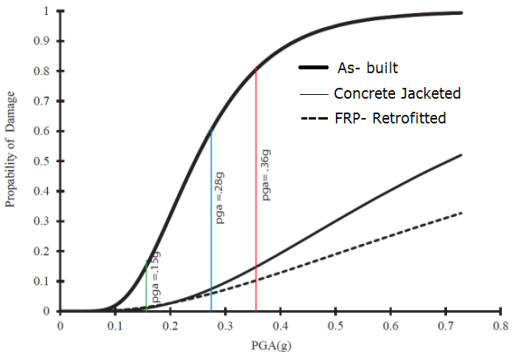

(b) moderate

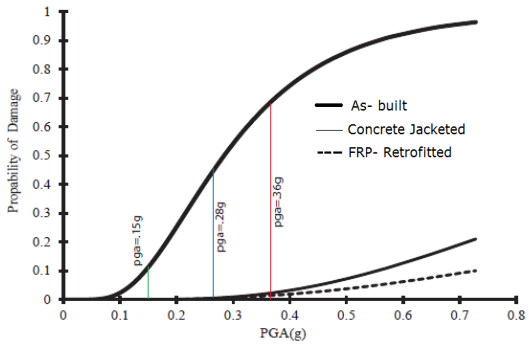

(c) extensive

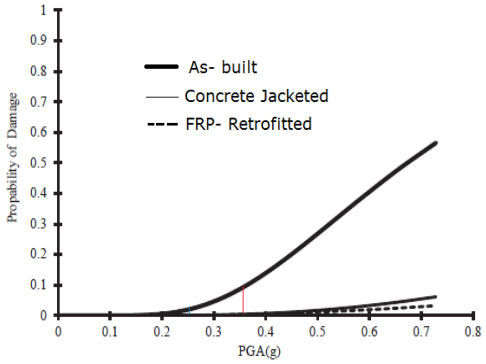

(d) collapse

Figure 9: Fragility curves of the overpass pier for different damage states

5.0 Conclusions

Seismic safety assessment of Abdul Mannan overpass is analytically evaluated using the equivalent static method as suggested by Japan Road Association (JRA) considering the different modes of failure. The lateral strength in bending has been obtained using the results of nonlinear sectional analysis of each pier section of the overpass, while the shear strength of the pier is estimated using the JRA recommended analytical expressions, taking into account the effect of depth, volumetric ratio of lateral steel, crushing strength of concrete, yield strength of steel. The moment-curvature relationship at the critical section of pier has been developed using the fiber model with conventional constitutive models for concrete and steel. The force-displacement relationship of each pier is derived by conducting pushover analyses of pier considering material and geometrical nonlinearities. The lateral seismic force, allowable lateral force, yield displacement, ultimate

displacement and displacement ductility are subsequently obtained for the overpass. The seismic safety of piers of the overpass is evaluated using the ductility method for ground motion intensities of PGA 0.15g and 0.25g.

From the numerical results it has been found that the most of the piers demonstrate bending mode of failure except two piers in which the shear mode of failure is dominated. The numerical results of the study indicate that most of the piers of the overpass do not comply the seismic safety requirements for design earthquake ground motion rerecords, which warrants the retrofit of piers of the overpass. Finally, an assessment of seismic retrofit strategy suitable for the overpass has been carried out. In this regard, the fragility curves of a typical overpass pier are derived for two retrofit techniques, such as FRP and concrete jacketing, in '*as built*' and '*retrofitted*' conditions for different damage states. In general, the '*retrofitted*' overpass pier has shown less susceptibility for each damage state in compared to that in '*as built*' condition. For each damage state of the overpass pier, the concrete jacketed pier has shown the higher damage susceptibility in compared to the FRP jacketed pier, at each level of ground motion intensity. In particular, the FRP and concrete jacketed overpass piers do not experience extensive and collapse states of damage, for the two ground motion intensities (PGAs of 0.15g and 0.25g); however, a considerable damage is seen to have incurred in the '*as built*' overpass. The numerical results as focused in the paper are expected to be helpful for the concerned authority of the city for taking initiatives in making the '*as built*' overpass as strong as necessary by selecting a proper retrofit strategy for withstanding the design seismic loads.

6.0 Acknowledgments

The authors sincerely acknowledge the support provided by Chittagong Development Authority (CDA) in supplying the *as-built* drawings and the associated geometric information of the overpass.

References

AASHTO (2002).*LRFD Bridge Design Specifications*, American Association of State Highway and Transportation Officials, 2nd ed., Washington, D.C., USA.

Akhter, S. H. (2010). *Earthquake of Dhaka*, A report on Seismicity of Bangladesh

Alam, M. Shahria, · Bhuiyan, M. A. Rahman and Billah, A. H. M. Muntasir (2012). *Seismic fragility assessment of SMA-bar restrained multi-span continuous highway bridge isolated by different laminated rubber bearings in medium to strong seismic risk zones.* Bulletin of Earthquake Engineering, 10:1885–1909.

Ali, M. H. and J. R. Choudhury. 1992. *Tectonics and earthquake occurrence in Bangladesh.* Proc. of the 36th Annual Convention of the Institution Engineers, Bangladesh, Dhaka

Alim, H., (2014). *Reliability based seismic performance analysis of retrofitted concrete bridge bent*, M. Engineering Thesis, Department of Civil Engineering, Chittagong University of Engineering and Technology (CUET), Chittagong, Bangladesh.

Applied Technology Council (ATC) (1985). *Earthquake damage evaluation data for California*, Report No. ATC-13, Applied Technology Council.

Bangladesh National Building Code (BNBC), (2006). House Building Research Institute, Dhaka, Bangladesh.

Basöz, N., Kiremidjian, A.S., King, S.A., and Law, K.H., (1998). *Statistical analysis of bridge damage data from the 1994 Northridge, CA, Earthquake,* Earthquake Spectra, 15: 25-53.

Bhuiyan, A.R., (2009). *Rheology modeling of laminated rubber bearings*, PhD dissertation, Graduate School of Science and Engineering, Saitama University, Japan

Bhuiyan, M. A. Rahman and Alam, M. Shahria (2012). *Seismic vulnerability assessment of a multi-span continuous highway bridge fitted with shape memory alloy bars and laminated rubber bearings*. Earthquake Spectra, 28(4):1379–1404.

Billah, A. H.M. Muntasir, Alam, M. S. and Bhuiyan, M. A. R., (2013). *Fragility analysis of retrofitted multi-column bridge bent subjected to near fault and far field ground motion*, ASCE Journal of Bridge Engineering, 108(10): 992-1004.

Caltrans. (1999). *Bridge design specifications manual,* California Department of Transportation, Sacramento, CA., USA.

Choi, E., DesRoches, R. and Nielson, B.G., (2004). *Seismic fragility of typical bridges in moderate seismic zones,* Engineering Structures, 26: 187-199

Cornell, A. C., Jalayer, F., Hamburger, R. O., (2002). *Probabilistic basis for 2000 SAC Federal Emergency Management Agency steel moment frame guidelines*, ASCE Journal of Structural Engineering, 128(4):526-532.

Eurocode 8. (1998). *Design provisions for earthquake resistance of structures*, European Standards, Brussels.

Federal Emergency Management Agency (FEMA) (2003), *HAZUS-MH software*, Washington DC.

Ghobarah, A., and Ali, H. M., (1988). *Seismic performance of highway bridges*, Engineering Structures, 10(3):157–166.

Hoshikuma, J., Kawashima, K., Nagaya, K., and Taylor, A.W., (1997). *Stress-strain Model for reinforced concrete in bridge piers,* ASCE Journal of Structural Engineering, 123(5):624-633.

Hwang, H., Jernigan, J.B., and Lin, Y.-W., (2000). *Evaluation of seismic damage to Memphis bridges and highway systems.* ASCE Journal of Bridge Engineering, 5: 322-30.

Hwang, H., Liu, J.B., and Chiu Y.-H., (2001). *Seismic fragility analysis of highway bridges*, *MAEC Report: Project MAEC RR-4*. Urbana: Mid-America Earthquake Center.

Japan Road Association (JRA) (2002). *Specifications for highway bridges- Part V: Seismic design*, Japan Road Association ,Tokyo, Japan.

Karim, K.R. and Yamazaki, F., (2001). *Effect of earthquake ground motions on fragility curves of highway bridge piers based on numerical simulation*,Earthquake Engineering and Structural Dynamics, 30: 1839–1856.

Mackie, K. R, Stojadinovi¢, B., (2004). *Fragility curves for reinforced concrete highway overpass bridges,*Proc. of 13th World Conference on Earthquake Engineering, Paper No. 1553.

Madas, P., and Elnashai, A. S., (1992). *A new passive confinement model for transient analysis of reinforced concrete structures*, Earthquake Engineering and Structural Dynamics, 21: 409-431.

Nielson, B., and DesRoches, R., (2007a). *Seismic fragility curves for typical highway bridge classes in the Central and Southeastern United States.* Earthquake Spectra, 23: 615–633.

Nielson, B.G. and DesRoches, R.,(2007b),"Seismic fragility methodology for highway bridges using a component level approach", *Earthquake Engineering and Structural Dynamics*, 36, 823–839

Padgett, J.E., and DesRoches, R., (2008). *Methodology for the development of analytical fragility curves for retrofitted bridges.* Earthquake Engineering and Structural Dynamics, 37: 157-174.

Park, Y. J., and Ang, A. H. S., (1985). *Mechanistic Seismic Damage Model for Reinforced Concrete.* ASCEJournal of Structural Engineering, 111 (4): 722-739.

Response (2000). Manual for Windows Version.

SeismoStruct (2011). SeismoStruct help file. Available from www.seismsoft.com

Shinozuka, M, Feng, M.Q., Kim, H.-K., and Kim, S.-H.,(2000). *Nonlinear static procedure for fragility curve development.* Journal of Engineering Mechanics, 126: 1287-95

Spoelstra, M., and Monti, G., (1999). *FRP Confined Concrete Model.*ASCE Journal of Composites for Construction, 3:143-150.

Yamazaki, F., Motomura, H., and Hamada, T., (2000). *Damage assessment of expressway networks in Japan based on seismic monitoring*. Proc. of 12th World Conference on Earthquake Engineering, CD-ROM, 2000: Paper No. 0551.